DOI: 10.21776/ub.jpacr.2022.011.03.703 *J. Pure App. Chem. Res.*, **2022**, 11 (3), 207-213
30 December 2022

Synthesis of Microsheets $Bi_4Ti_3O_{12}$ and $Bi_4Ti_{2.95}V_{0.05}O_{12}$ via Molten NaCl-KCl Salt Method

Anton Prasetyo[1*], Andy Nur Muhammad Guntur[1], Suci Noerfaiqotul Himmah[1], Nur Aini[1], Usman Ali Rouf[1], Abdul Aziz[2]

[1]Department of Chemistry, Faculty of Science and Technology, Universitas Islam Negeri Maulana Malik Ibrahim Malang, Malang, Indonesia, 65144
[2] Department of Mathematics, Faculty of Science and Technology, Universitas Islam Negeri Maulana Malik Ibrahim Malang, Malang, Indonesia, 65144

[*]Corresponding email: anton@kim.uin-malang.ac.id

Received 29 August 2022; Accepted 30 December 2022

ABSTRACT

$Bi_4Ti_3O_{12}$ is a tri-layer Aurivillius member compound that was reported to have good photocatalytic properties. Metal element doping and morphological particle tuning are strategies to increase photocatalyst activity. In this research, the compound micro sheets $Bi_4Ti_3O_{12}$ and $Bi_4Ti_{2.95}V_{0.05}O_{12}$ were synthesized using molten NaCl/KCl salt. The diffractogram shows that the $Bi_4Ti_3O_{12}$ sample was successfully synthesized, however, there are still found impurities at the $Bi_4Ti_{2.95}V_{0.05}O_{12}$ sample. Micrographs showed that the morphology particle samples is. The results of UV-Vis DRS spectra calculation show that both samples have a band gap energy of ~2.97 eV.

Keywords: $Bi_4Ti_3O_{12}$, $Bi_4Ti_{2.95}V_{0.05}O_{12}$, molten salt synthesis, NaCl-KCl, micro sheets.

INTRODUCTION

Dye waste have given negative impacts on the environment, so an efficient dye waste treatment is needed to maintain the sustainability of environment. One of the potential methods that have good ability in handling dye waste is photocatalyst technology [1, 2]. Several compounds have been reported to have the properties as photocatalyst materials, one of those materials is the Aurivillius structure compound [3, 4]. The general formula of Aurivillius compounds is $[Bi_2O_2]^{2+}[A_{m-1}B_mO_{3m+1}]^{2-}$ which is arranged alternately between bismuth and pseudo-perovskite layers. Cation-*A* is occupied by monovalent, divalent, or trivalent cations, such as Na^+, Ca^+, Sr^{2+}, Ba^{2+}, Pb^{2+}, or Bi^{3+}, while cation-*B* is occupied by high valence cations, such as Ti^{4+}, Nb^{5+}, or Ta^{5+}. The number of layer in Aurivillius is indicated by the number of pseudo perovskite layers denoted by "*m*" which is an integer number [5]. The advantage of Aurivillius compound as a photocatalyst material is caused by its ferroelectric properties that lead to reduce the rate of electron-holes recombination so that increasing photocatalytic activity [6]. In addition, the valence band of Aurivillius structure that involving electrons in the O 2*p* and Bi 6*s* orbitals is reported to increase photocatalytic activity [7].

The $Bi_4Ti_3O_{12}$ compound is classified as a tri-layers Aurivillius compound which has been reported to be potentially used as photocatalyst material with a band gap energy of 2.96 eV (419 nm) [8]. Meanwhile, some researchers reported that metal doping such as Fe or Cr on $Bi_4Ti_3O_{12}$ compounds can increase its visible light absorption [9, 10]. Therefore, the $Bi_4Ti_3O_{12}$ photocatalyst can use a wider visible light range advantageously as an excitation source. The

The journal homepage www.jpacr.ub.ac.id
p-ISSN : 2302 – 4690 | e-ISSN : 2541 – 0733

use of vanadium as metal doping on photocatalysts material has been reported by several researchers. Li et al. (2020) have reported that the presence of vanadium doping on TiO_2 can reduce its band gap energy so it can work effectively under visible light [11]. It indicates that vanadium metal has the potency to be used in reducing the band gap energy of $Bi_4Ti_3O_{12}$.

The particle morphology of $Bi_4Ti_3O_{12}$ has been reported to have an influence on its photocatalytic activity. Previous research reported that the plate-like particle of $Bi_4Ti_3O_{12}$ has a good photocatalytic activity [12, 13]. In addition, Chen et al. (2016) state that $Bi_4Ti_3O_{12}$ with nanosheet morphology has a good ability to degrade rhodamine B due to the high number of actives sites on its surface which can inhibit the rate of electron (e^-)-hole (h^+) recombination [13]. It indicated that the sheet/plate-like $Bi_4Ti_3O_{12}$ can provide more advantageous properties as a photocatalyst compound.

The molten salt method (MSS) is one of the simplest methods that can produce a unique particle morphology. This method has several advantages including (a) cheap, (b) environmentally friendly, and (c) lower synthesis temperature compared to the solid-state reaction method [14]. The synthesis of $Bi_4Ti_3O_{12}$ using the MSS method has been reported by many researchers [15, 16]. Moreover, Liu et al. (2017) have reported that they have succeeded in synthesizing the Fe-doped $Bi_4Ti_3O_{12}$ compound using the MSS method and obtained a nanosheet morphology that has a good photocatalytic activity [18]. It indicates that the MSS method can be used in metal-doped $Bi_4Ti_3O_{12}$ synthesis and obtained the nanosheet morphology that can increase its photocatalytic activity. Based on the description above, in this research, we synthesized vanadium doped $Bi_4Ti_3O_{12}$ using the MSS method and then, the phase, particle morphology, and band gap energy was characterized.

EXPERIMENT

Chemicals and Instrumentation

The precursors used in the synthesis of $Bi_4Ti_3O_{12}$ and $Bi_4Ti_{2.95}V_{0.05}O_{12}$ are Bi_2O_3 (Himedia, 99.9%), TiO_2 (Sigma Aldrich, 99.9%), and V_2O_3 (Sigma Aldrich, 99.9%). The other materials used are KCl (Merck, 99.5%), NaCl (Merck, 99.5%), $AgNO_3$ (Merck, 99.9%), and acetone (Merck).

The phase of synthesized compounds was identified using the *X*-ray diffraction (XRD) technique (Rigaku Miniflex diffractometer) with a measurement range 2θ (°) = 3-90. The particle morphology was obtained from characterization using scanning electron microscopy (SEM) (JEOL JSM-6360LA type). The obtained micrographs were processed using Image-J software to determine the particle size. The reflectance spectrum was obtained from measurements using ultraviolet-visible diffuse reflectance spectroscopy (UV-Vis DRS) (Thermo Scientific Evolution 220 spectrometer type) with a measurement range of 200-800 nm. The DRS spectra were analyzed using the Kubelka-Munk equation to calculate the band gap energy.

Procedure synthesis

3 grams of target compound was synthesized by NaCl-KCl (with ratio salt is 1:1) molten salt method with a molar ratio of the target compound and salt is 1:7. The precursors were weighed according to the stoichiometric calculations of the reaction. In the first stage, the precursors of Bi_2O_3, TiO_2, V_2O_3, and NaCl-KCl salt were ground in a mortar agate for an hour and during the grinding step, the small amount of acetone was added to make a homogeneous mixture. Then, the mixture of precursors and salt was calcined at temperatures 750 and 850°C for 6 hours. Finally, the obtained products was washed using hot water to remove the salt .The identification of the remaining NaCl-KCl salt was carried out by introducing $AgNO_3$ solution

into the aqueous waste of washing process. Furthermore, the sample was dried at a temperature of 75ºC.

RESULT AND DISCUSSION

The obtained product of $Bi_4Ti_3O_{12}$, and $Bi_4Ti_{2.95}V_{0.05}O_{12}$ are shown in Figure 1.It can be seen that the color of doped sample changed due to vanadium content. The sample of $Bi_4Ti_3O_{14}$ compound had white color, while the vanadium doped sample produced slightly yellowish color which indicated a chemical change occurred after doping.

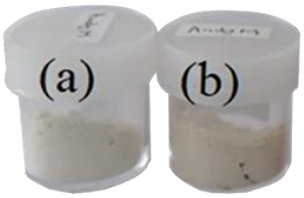

Figure 1. The sample of (a) $Bi_4Ti_3O_{12}$, and (b) $Bi_4Ti_{2.95}V_{0.05}O_{12}$

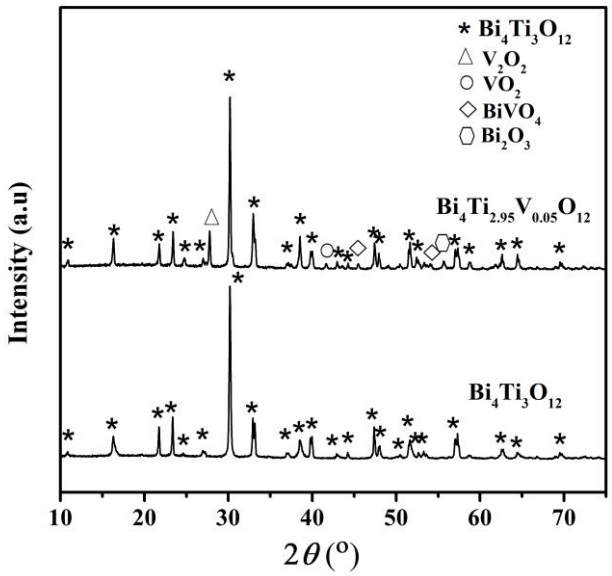

Figure 2. *X*-ray powder diffraction pattern of (a) $Bi_4Ti_3O_{12}$, and (b) $Bi_4Ti_{2.95}V_{0.05}O_{12}$

The *X*-ray diffraction pattern of sample of $Bi_4Ti_3O_{12}$, and (b) $Bi_4Ti_{2.95}V_{0.05}O_{12}$ are shown in Figure 2 and compared to the *X*-ray diffraction pattern standard of $Bi_4Ti_3O_{12}$ from Joint Committee on Powder Diffraction Standard (JCPDS) No. 35795. The comparison result showed that the $Bi_4Ti_3O_{12}$ and (b) $Bi_4Ti_{2.95}V_{0.05}O_{12}$ sample had conformity with the $Bi_4Ti_3O_{12}$ standard which was shown to have a typical diffraction peak at 2θ = 10.60, 16.20, 21.65, 23.14, 30.2, 32.80, 38.20, 47.18, 51.44, 57.08, 62.60, and 64.21˚. The impurities in the $Bi_4Ti_{2.95}V_{0.05}O_{12}$ sample were identified as: (a) Bi_2O_3 which was identified by the presence of peak 43.62, and 55.62˚ (JCPDS No. 006-0312) (b) V_2O_2 which was identified by the presence of peak 27.76˚ (JCPDS No. 019-1398) (c) VO_2 with the presence of peak 41.67˚ (JCPDS No. 033-1440), and (d) $BiVO_4$ with peak 45.46˚ (JCPDS No. 01-074-1721). The presence of Bi_2O_3 impurity indicates that the presence of unreacted precursor remained. Meanwhile, V_2O_2, VO_2, dan $BiVO_4$ impurities indicate that vanadium is difficult to replace the position of the Ti atom

in $Bi_4Ti_3O_{12}$ and tend to form another compound. Further look into the ionic radii *B*-cation, whereas the ionic radii of Ti^{4+} atom is 0.605 Å, and V^{3+} has a value of 0.640 Å [19]. It was a found small enough the difference therefore it can be replaced theoretically. However, the position of highest intensity peak is relative same and also there are found impurities. It indicates that the synthesis conditions still cannot cause V^{3+} metal to replace Ti^{4+} at *B*-site.

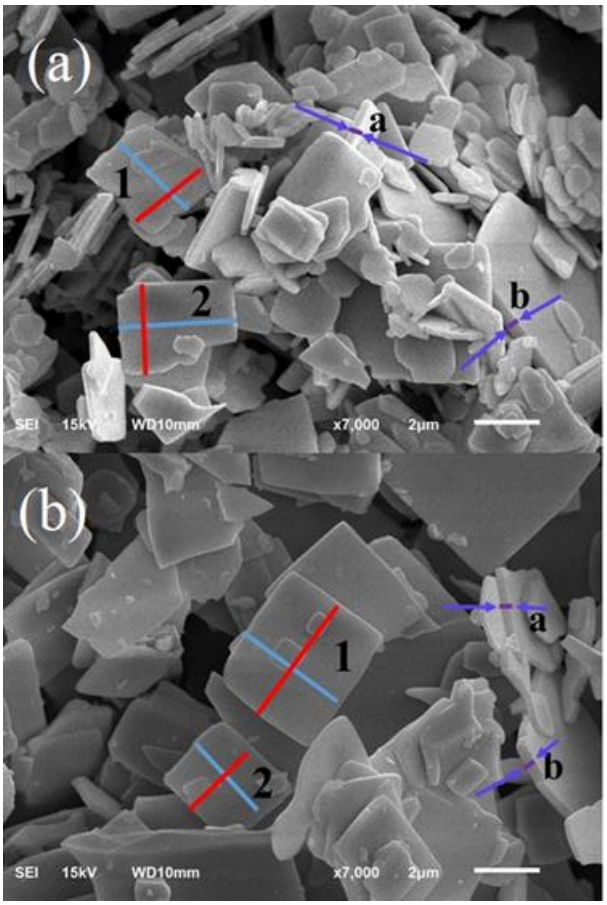

Figure 3. Particle morphology of (a) $Bi_4Ti_3O_{12}$, and (b) $Bi_4Ti_{2.95}V_{0.05}O_{12}$ (Red line denotes the length of particle; blue line indicates the width of particle and purple arrow denotes the thickness of particle)

Table 1 The particle size of (a) $Bi_4Ti_3O_{12}$, and (b) $Bi_4Ti_{2.95}V_{0.05}O_{12}$

Compound	Particle	Length (μm)	Width (μm)	Thickness (μm)
$Bi_4Ti_3O_{12}$	1	2.870	2.740	-
	2	3.550	2.773	-
	a	-	-	0.244
	b	-	-	0.407
$Bi_4Ti_{2.95}V_{0.05}O_{12}$	1	4.170	3.721	-
	2	3.028	2.614	-
	a			0.250
	b			0.339

The particle morphology of (a) $Bi_4Ti_3O_{12}$ and (b) $Bi_4Ti_{2.95}V_{0.05}O_{12}$ are shown in Figure 3 and it is known that the particle morphology of the synthesis product was in the form of micro sheets which is similar to work result that reported by Liu et al. (2017) [10]. However, it had a larger size in this study. The results of size calculation using the Image-J software are summarized in Table 1, and it can be seen that the obtaining particles had a length and width in the range of 2.614-4.170 μm, while the thickness measurement of selected particles was in the range of 0.224-0.407 μm. The large particle size indicates that the particle growth rate is greater than the rate of nucleation or crystal seed formation [15, 17].

The resulting particle size using the MSS method is also influenced by the composition of precursors because it affects the solubility of salt [14, 20]. Table 1 showed that the sample size of $Bi_4Ti_{2.95}V_{0.05}O_{12}$ had a larger size (length *x* width) than $Bi_4Ti_3O_{12}$ which indicated that the presence of V_2O_3 precursors affected the particle growth. The direction of particle growth was also different by comparing of sample thickness, namely the $Bi_4Ti_3O_{12}$ sample had a greater thickness and indicated that the $Bi_4Ti_3O_{12}$ particle growth tended to be upward (vertical) while the $Bi_4Ti_{2.95}V_{0.05}O_{12}$ sample tended to the side (horizontal).

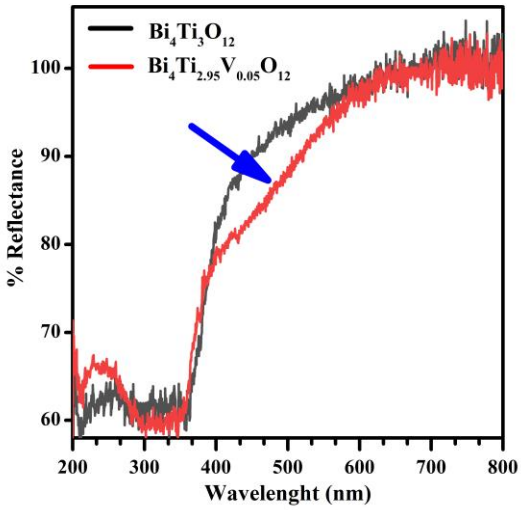

Figure 4. %Reflectance spectra of (a) $Bi_4Ti_3O_{12}$, and (b) $Bi_4Ti_{2.95}V_{0.05}O_{12}$

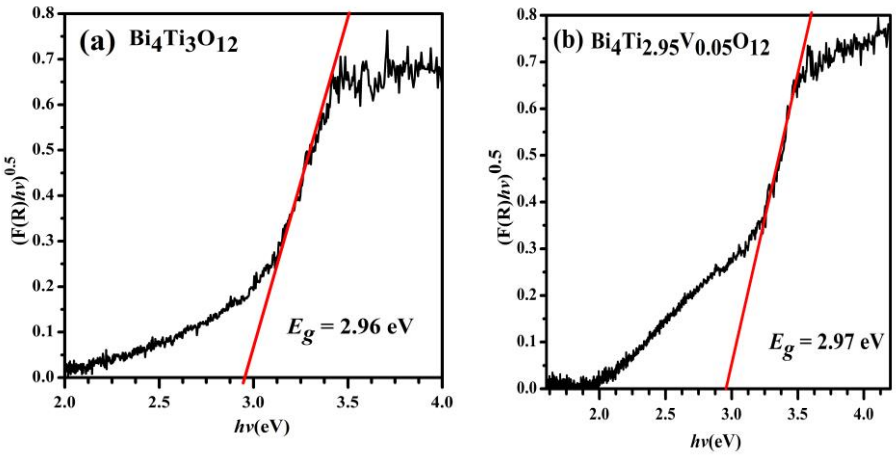

Figure 5. Tauc plot of (a) $Bi_4Ti_3O_{12}$, and (b) $Bi_4Ti_{2.95}V_{0.05}O_{12}$

Table 2. The band gap energy and absorption of (a) $Bi_4Ti_3O_{12}$, and (b) $Bi_4Ti_{2.95}V_{0.05}O_{12}$

Compound	Band gap energy (eV)
$Bi_4Ti_3O_{12}$	2.96
$Bi_4Ti_{2.95}V_{0.05}O_{12}$	2.97

The DRS spectra of $Bi_4Ti_3O_{12}$ and (b) $Bi_4Ti_{2.95}V_{0.05}O_{12}$ sample are shown in Figure 4, and it can be seen that reflectance slightly shifted to the visible light range. It's indicated that the presence of vanadium influenced to reflectance spectrum. DRS spectra sample was analyzed using the Kubelka-Munk equation and the Tauc plot are shown in Figure 5. The results of the band gap energy are tabulated in Table 2. The band gap energy of $Bi_4Ti_3O_{12}$ compounds has similarity with work result reported by Wang et al. (2020) [21]. The electronic transition that occurs in $Bi_4Ti_3O_{12}$ compounds involves electrons in the O 2*p* and Bi 2*s* orbitals which are occupied the valance band and electrons in the Ti 3d orbitals which are the conduction band [22]. The band gap energy of the $Bi_4Ti_{2.95}V_{0.05}O_{12}$ sample was slightly similar to $Bi_4Ti_3O_{12}$ sample and this related to the results of the *X*-ray diffraction pattern of samples which stated that the V^{3+} metal did not succeed in replacing Ti^{4+} so that there is no new electronic transitions formed.

CONCLUSION

The $Bi_4Ti_3O_{12}$ compound was successfully synthesized, meanwhile $Bi_4Ti_{2.95}V_{0.05}O_{12}$ did not formed. Impurities in $Bi_4Ti_{2.95}V_{0.05}O_{12}$ indicate that the vanadium has not been able to replace Ti cation partially. The obtaining particle morphology of $Bi_4Ti_3O_{12}$ and $Bi_4Ti_{2.95}V_{0.05}O_{12}$ were microsheets, and the sample containing vanadium had a larger size than undoped sample. In addition, the band gap energy of all samples are relative same.

ACKNOWLEDGMENT

This research was funded by the 2020 BOPTN Research Grant scheme, Institute for Research and Community Service (LP2M), Universitas Islam Negeri Maulana Malik Ibrahim Malang No DIPA BLU-DIPA 025.04.2.423812/2019.

REFERENCES

[1] Forgacs, E., Cserhati, T., and Orosb, G., *Environ. Int.*, **2004**, 30, 953–971.
[2] Anwer, H., Mahmood, A., Lee, J., Kim, K.H., Park, J.W., and Yip, A.C.K., *Nano Res.*, **2019**, 12, 5, 955-972.
[3] Zhu, Z., Wan, S., Zhao, Y., Gu, Y., Wang, Y., Qin, Y., Zhang, Z., Ge, X., Zhong, Q., and Bu, Y., *Materials Reports: Energy*, **2021**, 1, 100019.
[4] Rouf, U.A., Hastuti, E., and Prasetyo, A., *Jurnal Kartika Kimia*, **2021**, 4, 1, 51-57.
[5] Aurivillius, B. *Arkiv For Kemi*, **1949**, I, 54, 463-480.
[6] Khan, M. A., Nadeem, M. A. and Idriss, H., *Surf. Sci. Rep.*, **2016**, 71, 1, 1–31.
[7] Chen, P., Liu, H., Cui, W., Lee, S.C., Wang, L., and Dong, F., *EcoMat*, 2020, 2, 3, e12047
[8] Wang, Y., Zhang, X., Zhang, C., Li, R., Wang, Y., and Fan, C., *Inorg. Chem. Commun.*, **2020**, 116, 107931.
[9] Chen, Z., Jiang, X., Zhu, C., and Shi, C., *Appl. Catal. B.*, **2016**, 199, 241–251.
[10] Liu, Y., Zhu, G., Gao, J., Hojamberdiev, M., Zhu, R., Wei, X., Guo, Q., and Liu, P., *Appl. Catal. B.*, **2017**, 200, 72-82.

[11] Li, H., Zhao, G., Chen, Z., Han, G., and Song, B., *J. Colloid Interface Sci.*, **2010**, 344, 247–250.
[12] Zhao, W., Jia, Z., Lei, E., Wang, L., Li, Z., and Dai, Y., *J. Phys. Chem. Solids.*, **2013**, 74, 1604-1607.
[13] Chen, Z., Jiang, H., Jin, W., and Shi, C., *Appl. Catal. B.*, **2016**, 180, 698-706.
[14] Kimura, T. 2011, Molten salt synthesis of ceramic powders. *Advances in Ceramics Synthesis and Characterization, Processing and Specific Applications*. Rijeka: In Tech.
[15] Zhao, Z., Li, X., Ji, H., and Deng, M., *Integr. Ferroelectr.*, **2014**, 154, 54–158.
[16] Januari T., Aini N., Barorroh H., Prasetyo A., *IOP Conf. Ser.: Earth Environ. Sci*. 2020, 456: 012013.
[17] Marela, S.D., Aini, N., Hardian, A., Suendo, V., and Prasetyo, A., *J. Pure App. Chem. Res.*, **2021**, 10, 1, 64-71
[18] Liu, Y., Zhu, G., Gao, J., Hojamberdiev, M., Zhu, R., Wei, X., Guo, Q., and Liu, P., *Appl. Catal. B.*, **2017**, 200, 72-82.
[19] Shannon, R. D. 1976. *Acta Crystallogr.*, 1976, A32, 751-767.
[20] H. Maulidianingtiyas, A. D. Prasetiyo, F. Haikal, I. N. Cahyo, V. N. Istighfarini, and A. Prasetyo., *Alchemy Jurnal Penelitian Kimia*, **2021**, 17, 2, 211-218.
[21] Wang, Y., Zhang, X., Zhang, C., Li, R., Wang, Y., and Fan, C., *Inorg. Chem. Commun.*, 2020, 116, 107931.
[22] Lardhi, S., Noureldine, D., Harb, M., Ziani, A., Cavallo, L., and Takanabe, K., *J. Chem. Phys.*, **2016**, 144, 134702.